Introduction to nanotechnology:

Chapter 4 : Properties of Nanoparticles

Yang-Yuan Chen陳洋元中研院物理所
Low temperature and nanomaterial labatory
Institute of Physics, Academia Sinica
中興大學物理系
E-mail : Cheny2@phys.sinica.edu.tw
http://www.phys.sinica.edu.tw/%7Elowtemp/

Introduction:

1. **Metal Nanoclusters**
2. **Semiconducting Nanoclusters**
3. **Rare Gas and Molecular Clusters**
4. **Methods of Synthesis**

4 Properties of Individual Nanoparticles

Nanoparticles

- size? ~ 1-1000 nm
- Criterion: Critical length or characteristic length
- 1. Thermal diffusion length
- 2. Scattering length (mean free path)
- 3. Coherence length
- 4. Energy level spacing >> thermal energy KT
- 5. Surface effect
- 6. other

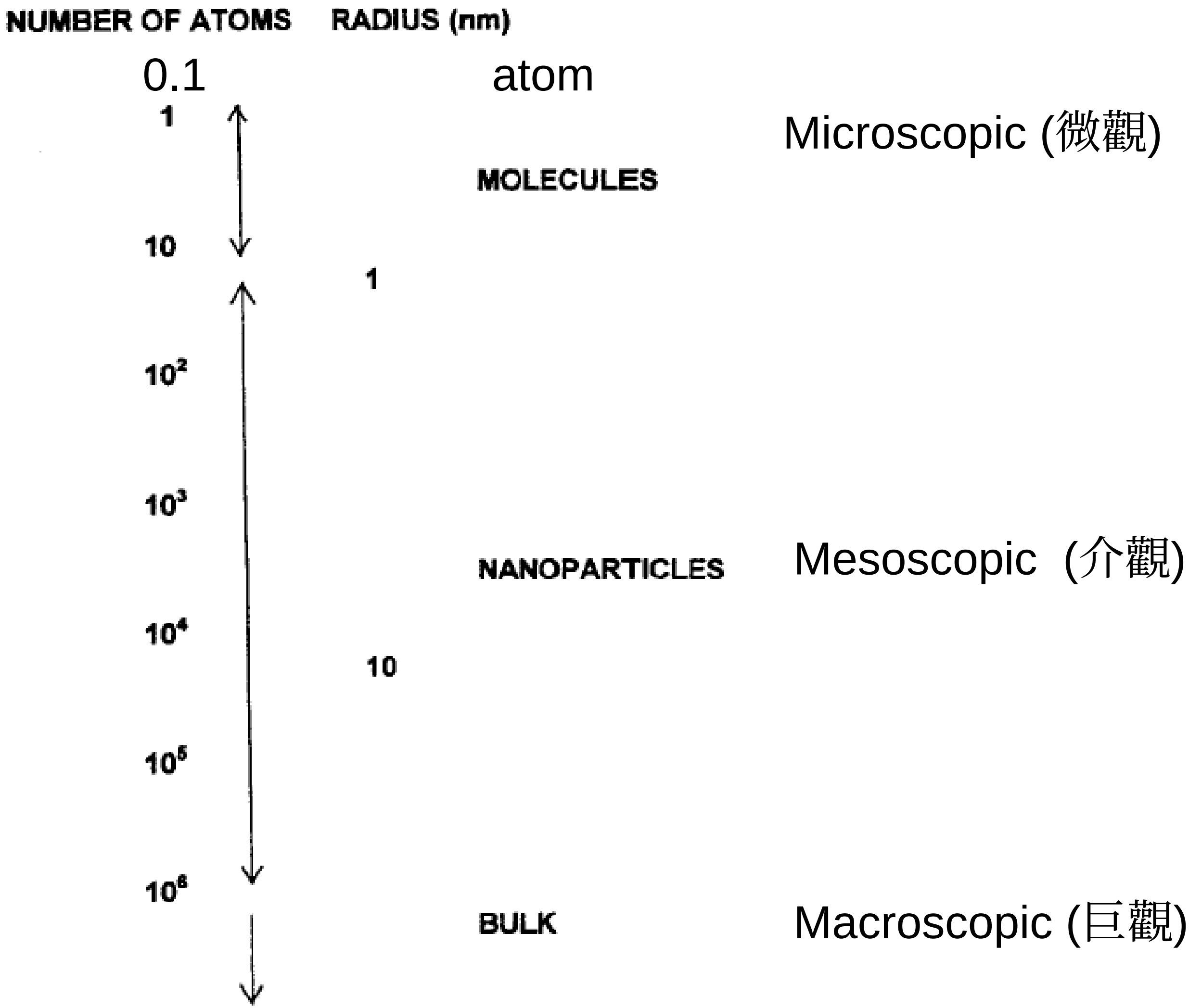

Figure 4.1. Distinction between molecules, nanoparticles, and bulk according to the number of atoms in the cluster.

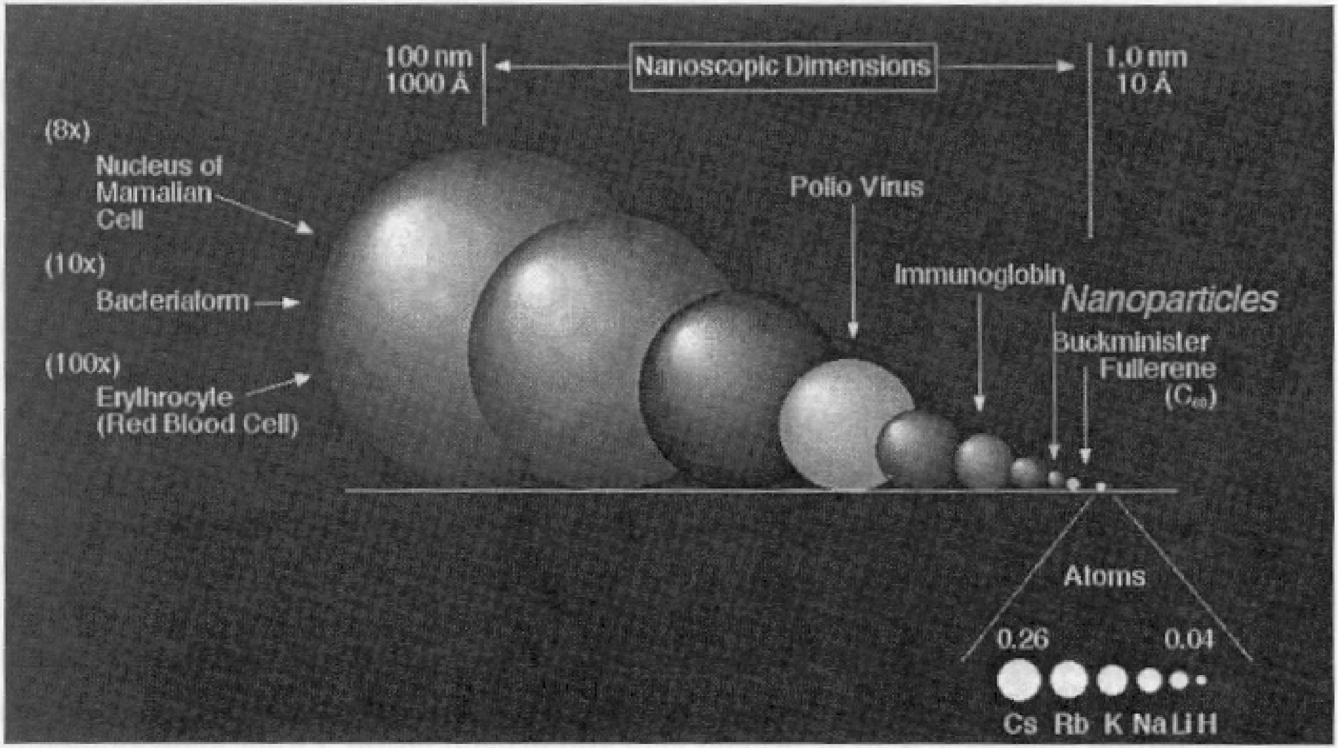

FIGURE 1.2 Size comparisons of nanocrystals with bacteria, viruses, and molecules.

病毒 Virus ~10 nm~100 nm

紅血球 blood cell 200~300 nm

細菌 bacteria 200~600 nm

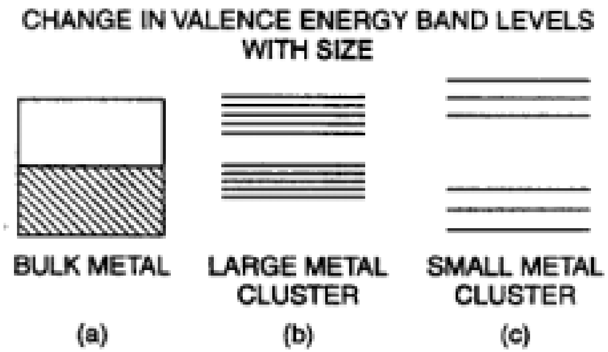

Figure 4.9. Illustration of how energy levels of a metal change when the number of atoms of the material is reduced: (a) valence band of *bulk metal*; (b) *large metal cluster* of 100 atoms showing opening of a band gap; (c) *small metal cluster* containing three atoms.

Energy

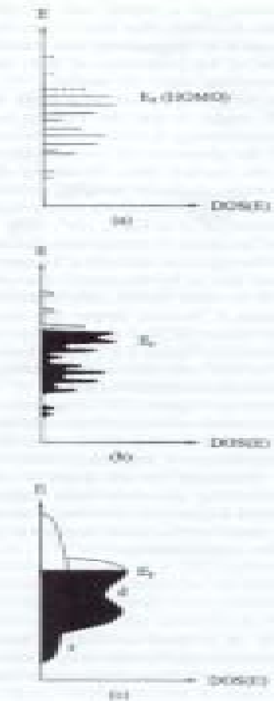

... 2.2 Formation of a band structure (a) from a molecular state, (b) from a ... with broadened energy states, and (c) the fully developed band structure ... E_F = Fermi energy; DOS = density of states. In (a) E_F corresponds to ... molecular orbital (HOMO).

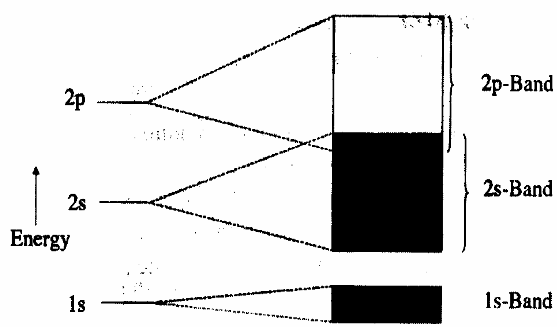

FIGURE 2.3 Overlap of the fully occupied 2*s* band with the empty 2*p* band in beryllium is responsible for the metallic behavior.

do 2D and 1D arrangements.

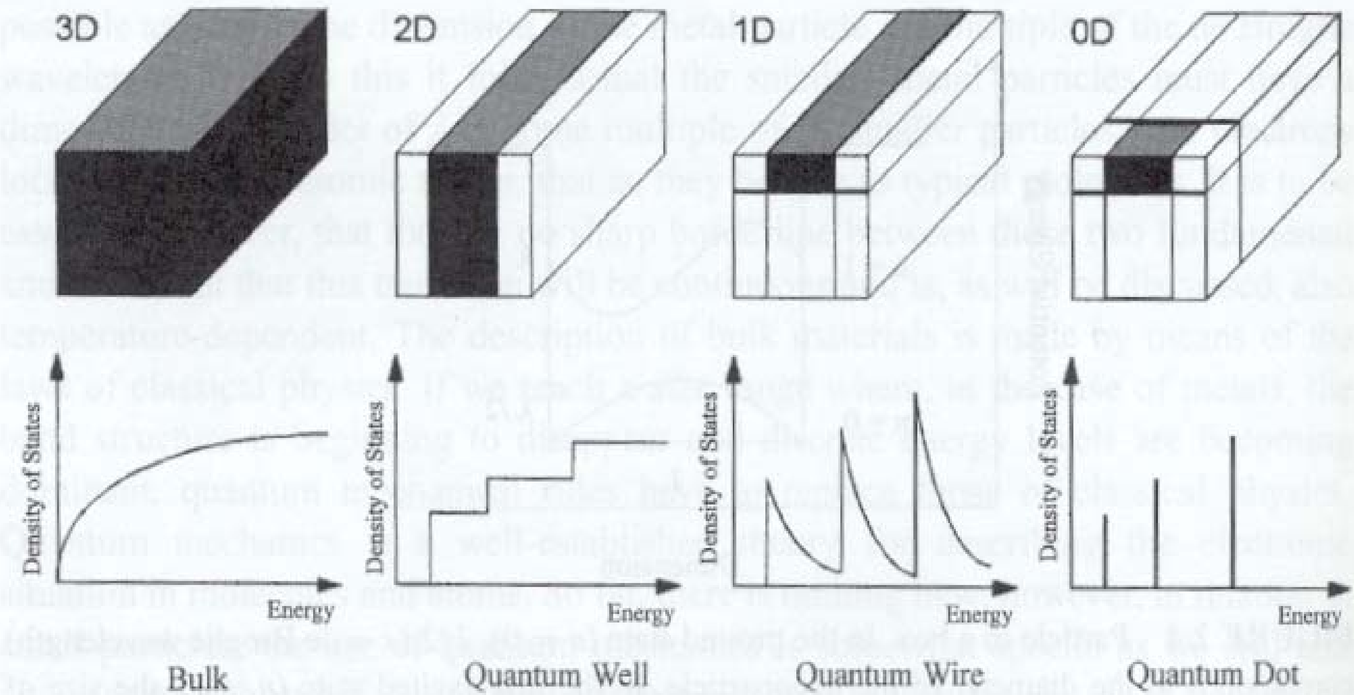

Surface effect

TABLE 2.1 The relation between the total number of atoms in full shell clusters and the percentage of surface atoms

Full-shell Clusters		Total Number of Atoms	Surface Atoms (%)
1 Shell		13	92
2 Shells	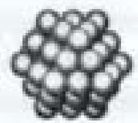	55	76
3 Shells	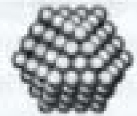	147	63
4 Shells		309	52
5 Shells		561	45
7 Shells	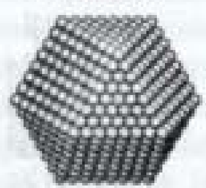	1415	35

With FCC structure

4.2.1 Magic numbers and structure

No. of electrons for an atom:
electronic magic numbers example

He2: $1S^2$
Ne10: $1S^2, 2S^2, 2P^6$
Ar 18: $1S^2, 2S^2, 2P^6, 3S^2, 3P^6$,
Kr 36: $1S^2, 2S^2, 2P^6, 3S^2, 3P^6$,
$3d^{10}$

2. No. of atoms for a nanoparticles
   Structural magic number

   The jellium model P75

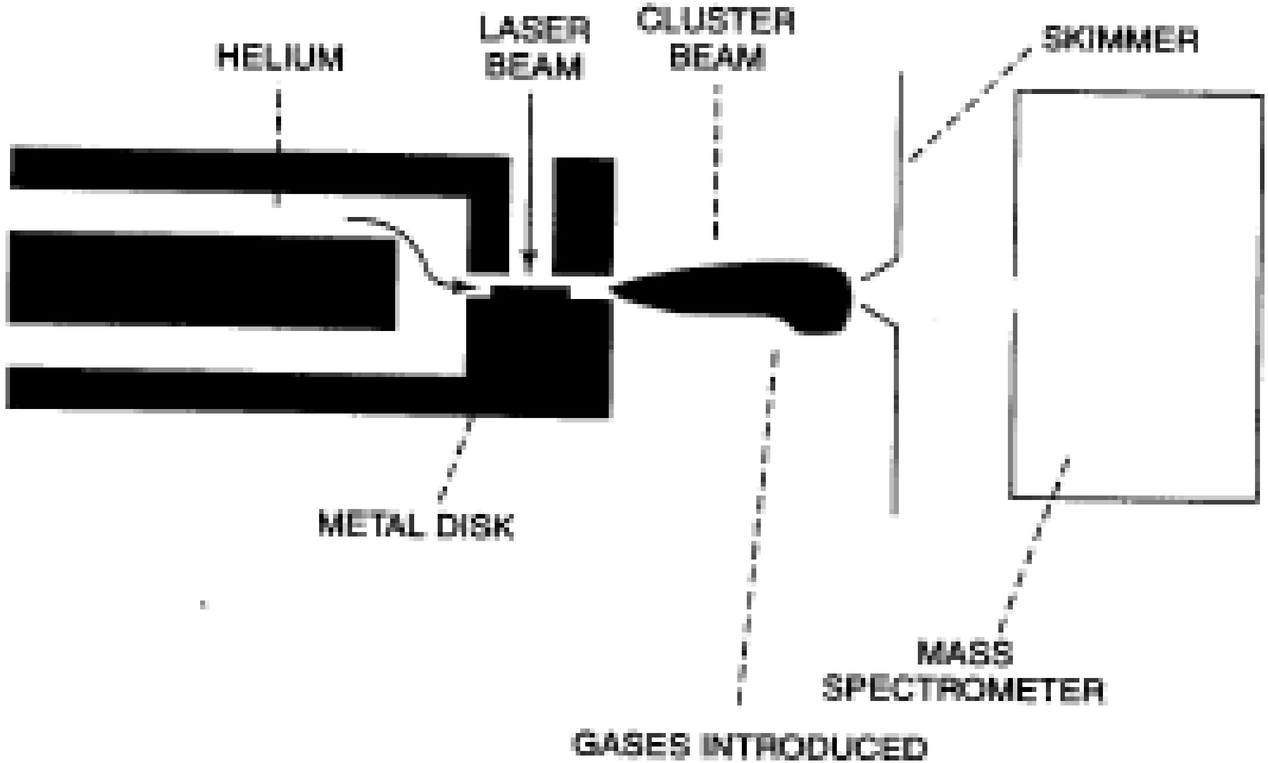

Figure 4.2. Apparatus to make metal nanoparticles by laser induced evaporation of atoms from the surface of a metal. Various gases such as oxygen can be introduced to study the chemical interaction of the nanoparticles and the gases. (With permission from F. J. Owens and C. P. Poole, Jr., *New Superconductors*, Plenum Press, 1999.)

準分子雷射濺鍍 (Excimer Laser Ablation簡稱 ELA)**(建於2003/3)**
及奈米成長真空系統**(建於1993/1)**。

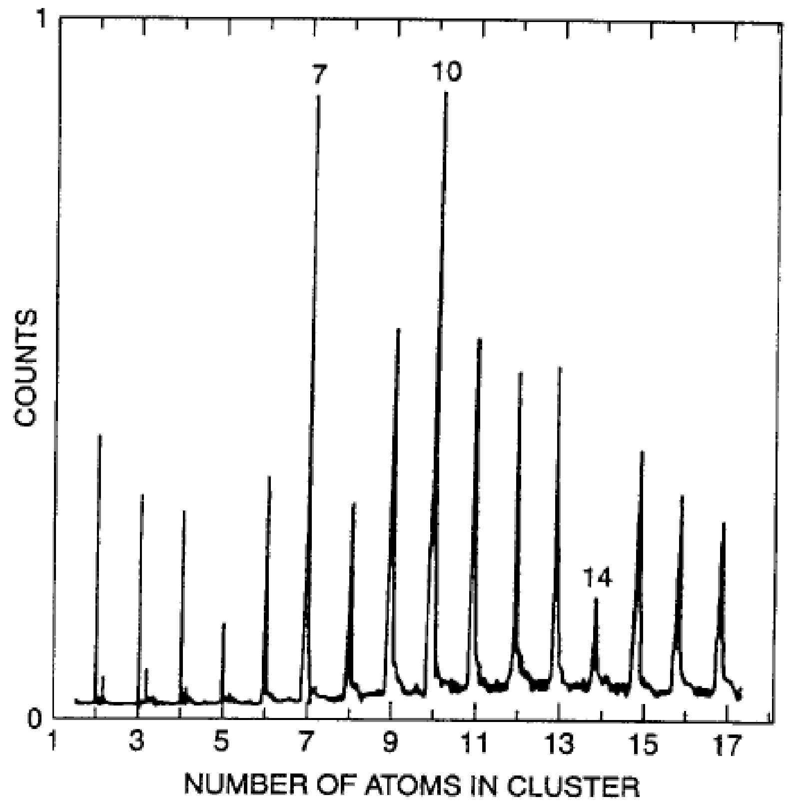

Figure 4.3. Mass spectrum of Pb clusters. [Adapted from M. A. Duncan and D. H. Rouvray, *Sci. Am.* 110 (Dec. 1989).]

4.2.2 Theoretical Modeling of Nanoparticles

Electronic magic numbers: the total mumber of electrons on the superatom when the top level is filled

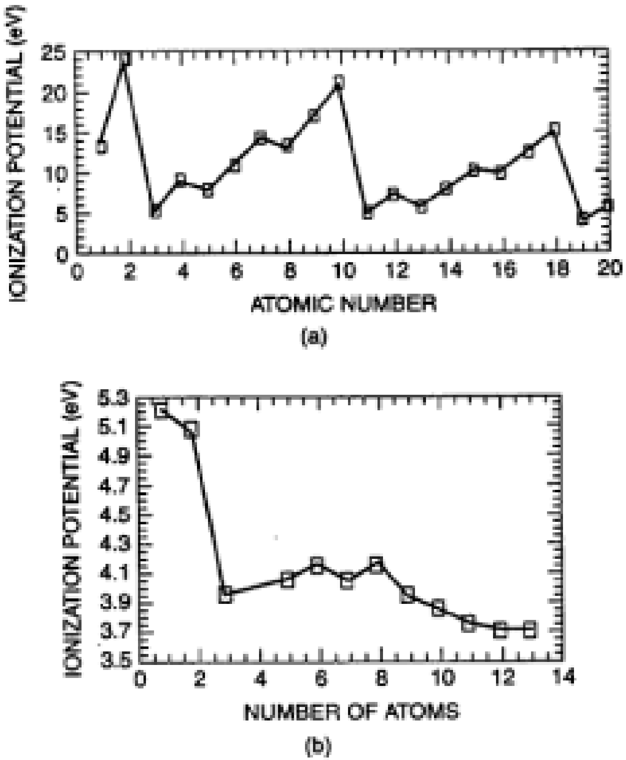

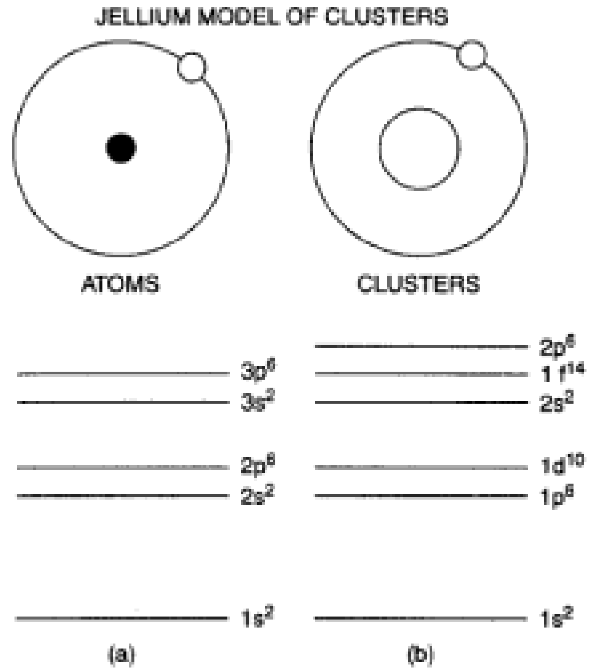

The jellium model   P75

Structural magic number:Cluster has a size in which all the energy levels are filled

Theoretical calculation:Cluster as molecular

- Molecular orbital theory P78
- Density functional theory P78

$$\psi(1s) = A\exp\left(-\frac{r}{\rho}\right) \tag{4.1}$$

the H_2^+ ion, molecular orbital theory assumes that the wavefunction of the electron around the two H nuclei can be described as a linear combination of the wavefunction of the isolated H atoms. Thus the wavefunction of the electrons in the ground state will have the form,

$$\psi = a\psi(1)_{1s} + a\psi(2)_{1s} \tag{4.2}$$

The Schrödinger equation for the molecular ion is

$$\left[\left(\frac{-\hbar^2}{2m}\right)\nabla^2 - \frac{e^2}{r_a} - \frac{e^2}{r_b}\right]\psi = E\psi \tag{4.3}$$

Find the structure and geometry with the lowest energy

4.2.3 Geometric Structure

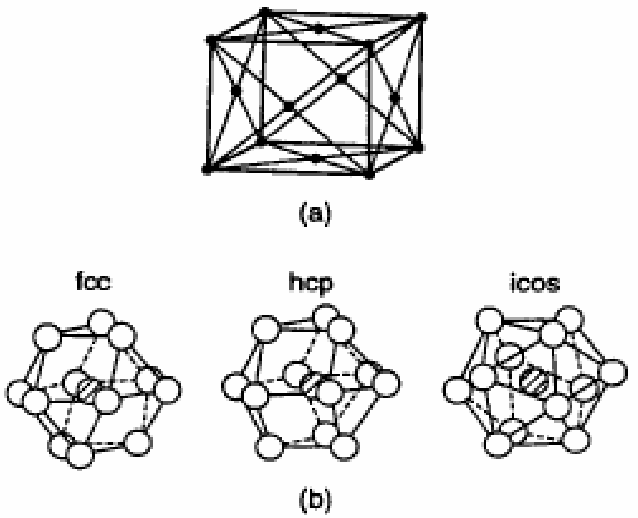

Figure 4.6. (a) The unit cell of bulk aluminum; (b) three possible structures of Al_{13}: a face-centered cubic structure (FCC), an hexagonal close-packed structure (HCP), and an icosahedral (ICOS) structure.

Table 4.1. Calculated binding energy per atom and atomic separation in some aluminum nanoparticles compared with bulk aluminum

Cluster	Binding Energy (eV)	Al Separation (Å)
Al_{13}	2.77	2.814
Al_{13}^{-}	3.10	2.75
Bulk Al	3.39	2.86

Size dependent structure of Indium nanoparticles

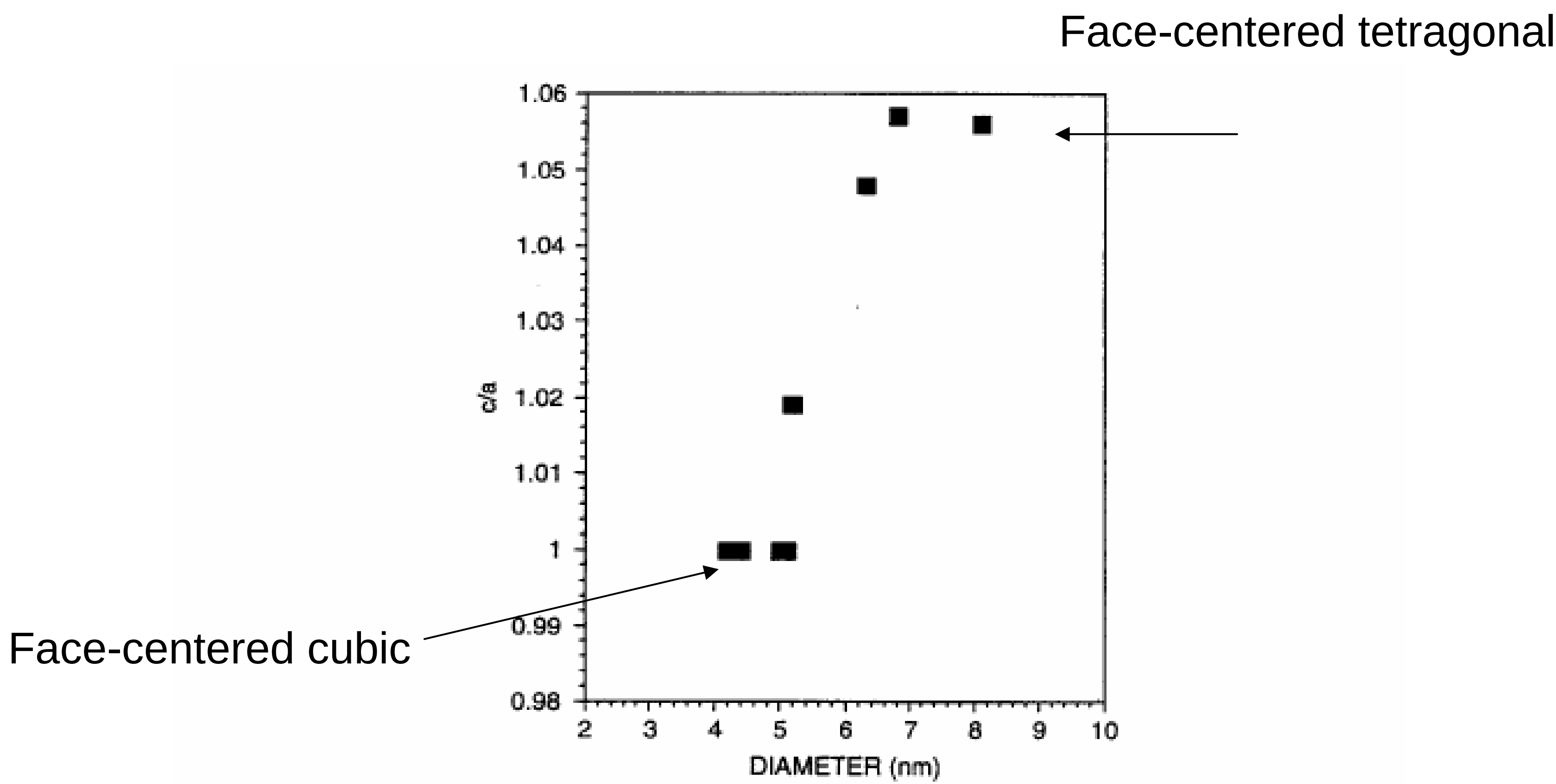

Figure 4.7. Plot of the ratio of the length of the *c* axis to the *a* axis of the tetragonal unit cell of indium nanoparticles versus the diameter of nanoparticles. [Plotted from data in A. Yokozeki and G. D. Stein, *J. Appl. Phys.* **49**, 224 (1978).]

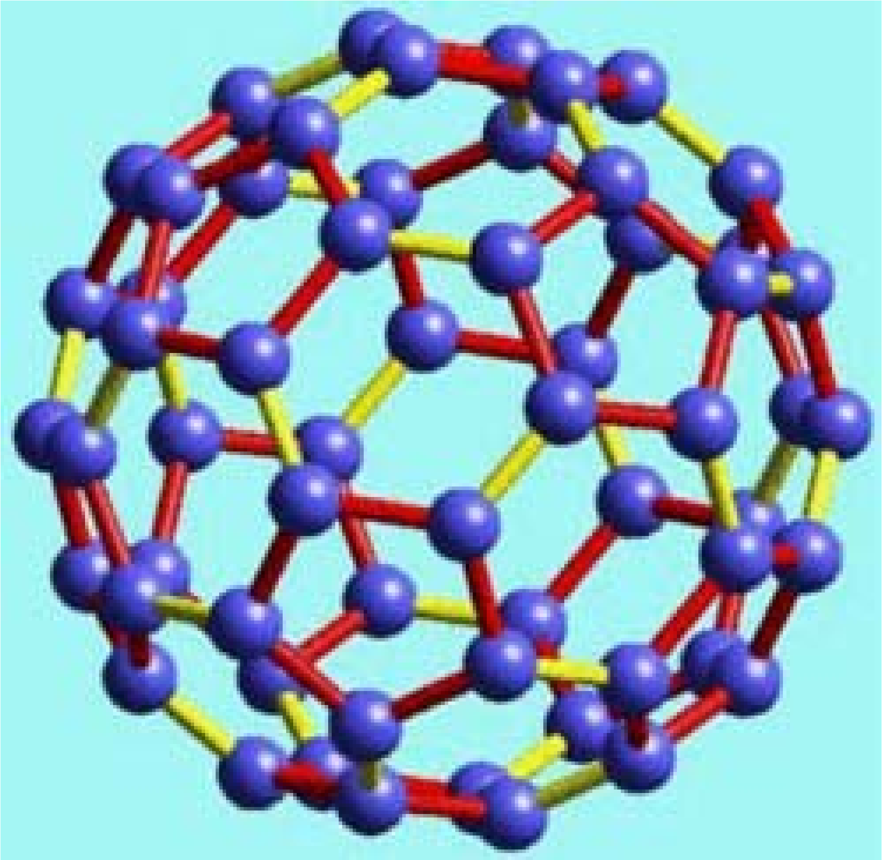

Magic number：C_{20}, C_{24}, C_{28}, C_{32}, C_{36}, C_{50}, C_{60}, C_{70}

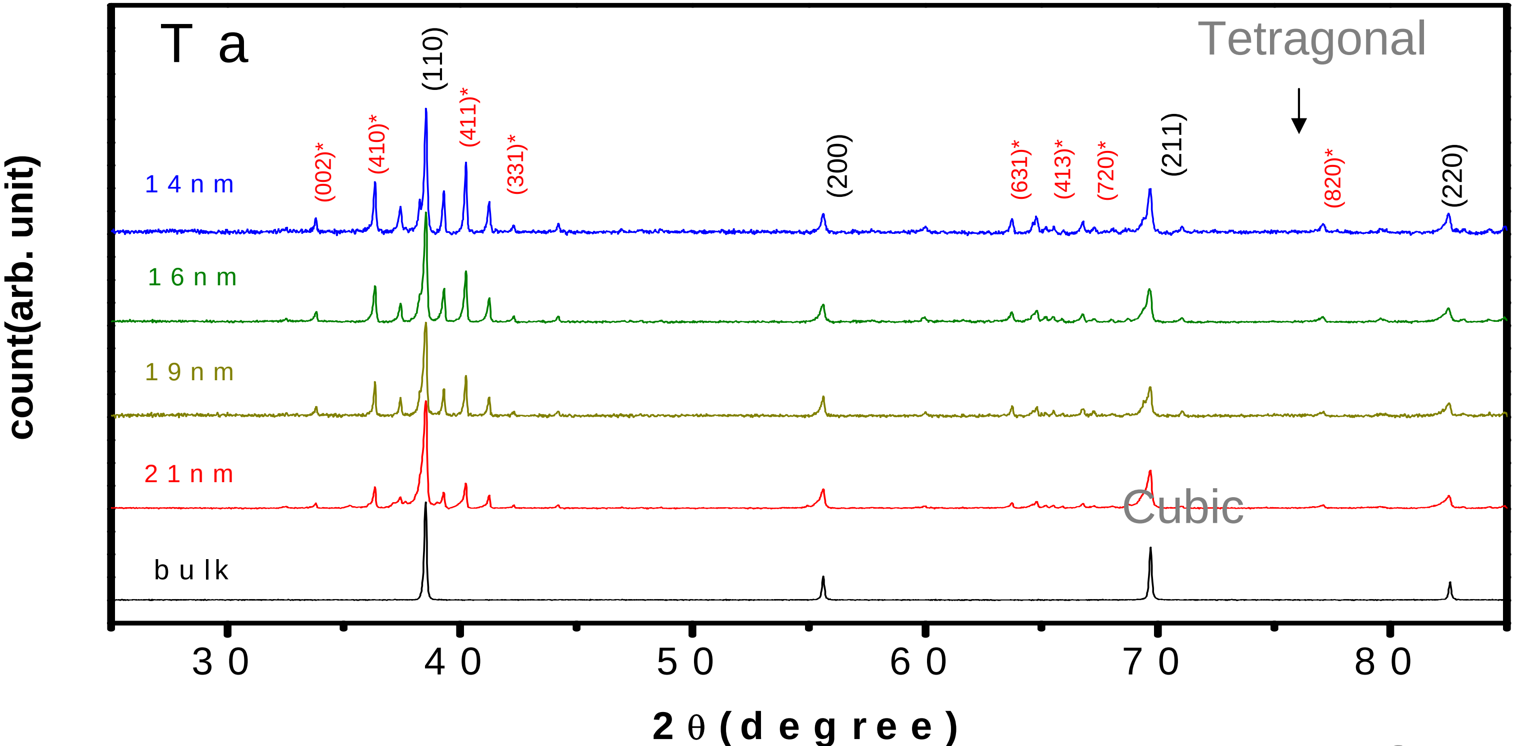

X –ray spectra of Ta

Size (nm)	α-Ta (%) Cubic	β- Ta (%) Tetragonal
14	42.4	57.6
16	44.7	55.3
19	47.8	52.2
21	66.7	33.3
bulk	100	0

彭翊凱 陳致文

Size dependence of phase compositions

lattice constant of Ta

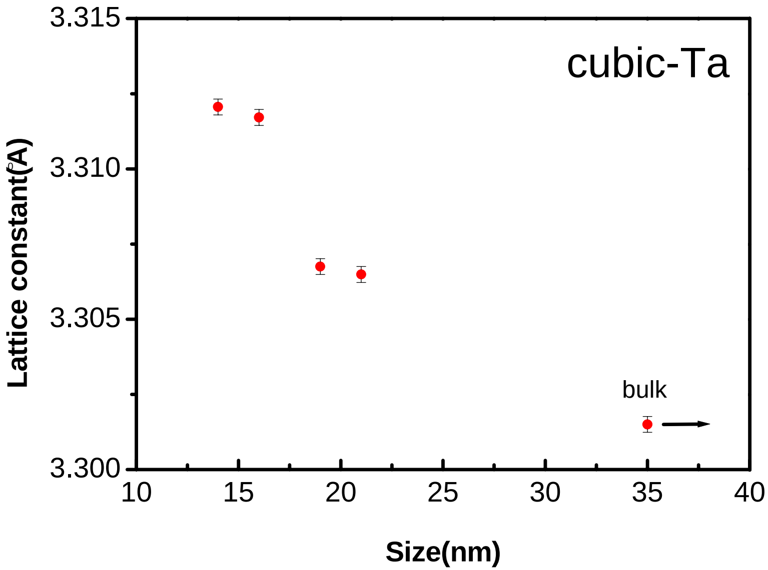

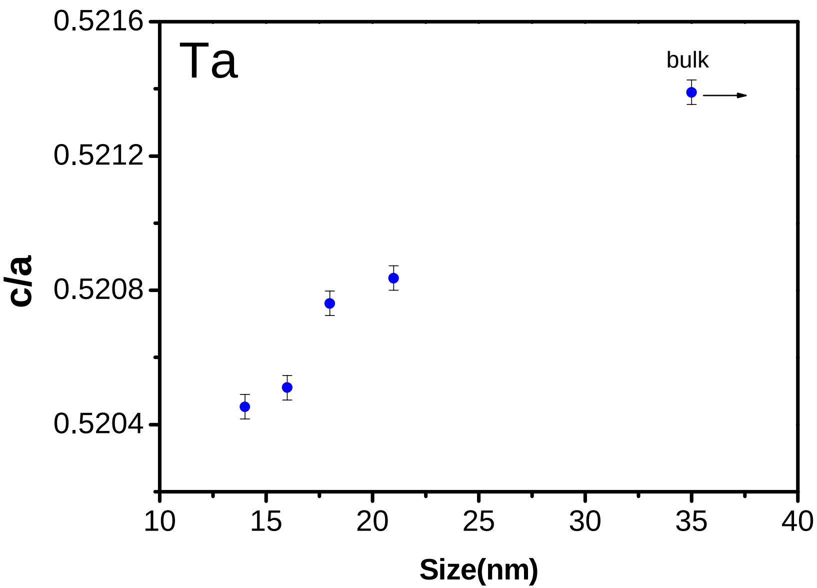

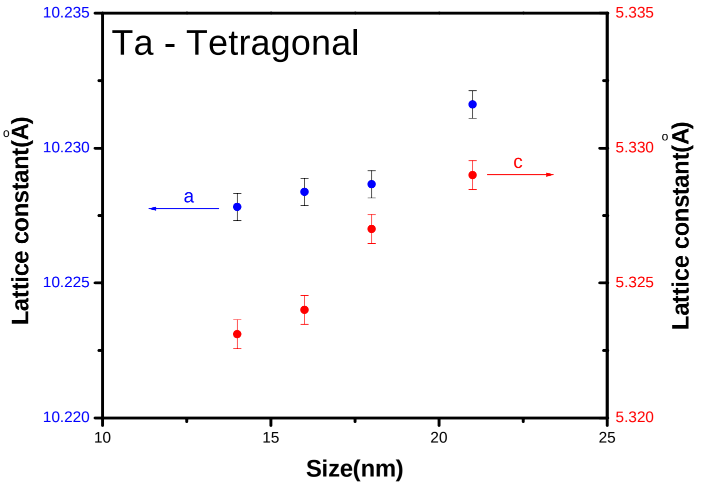

4.2.4 Electronic Structure

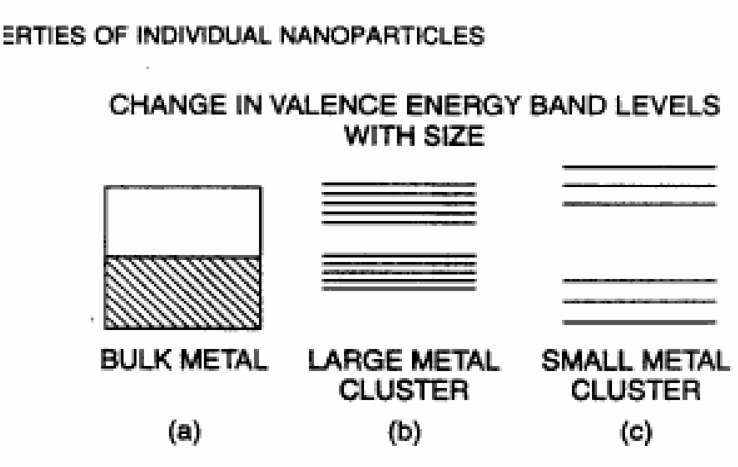

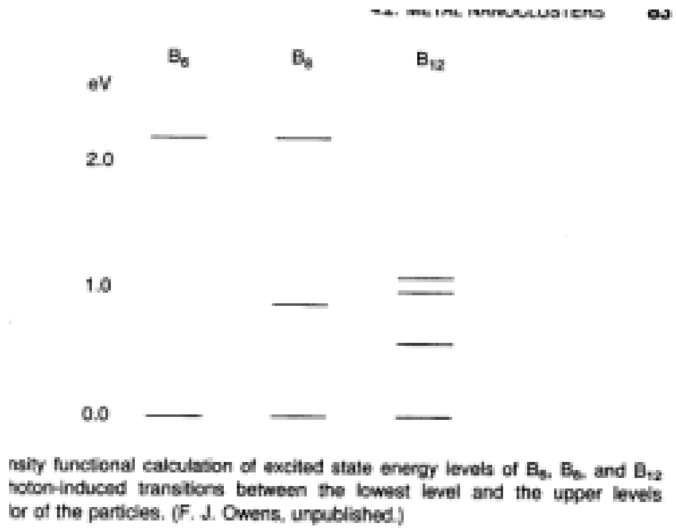

Bulk 100 atoms 3 atoms

Quantum Size Effect :
Energy level spacing >> $K_B T$

Light-induced transitions between these levels determines the color

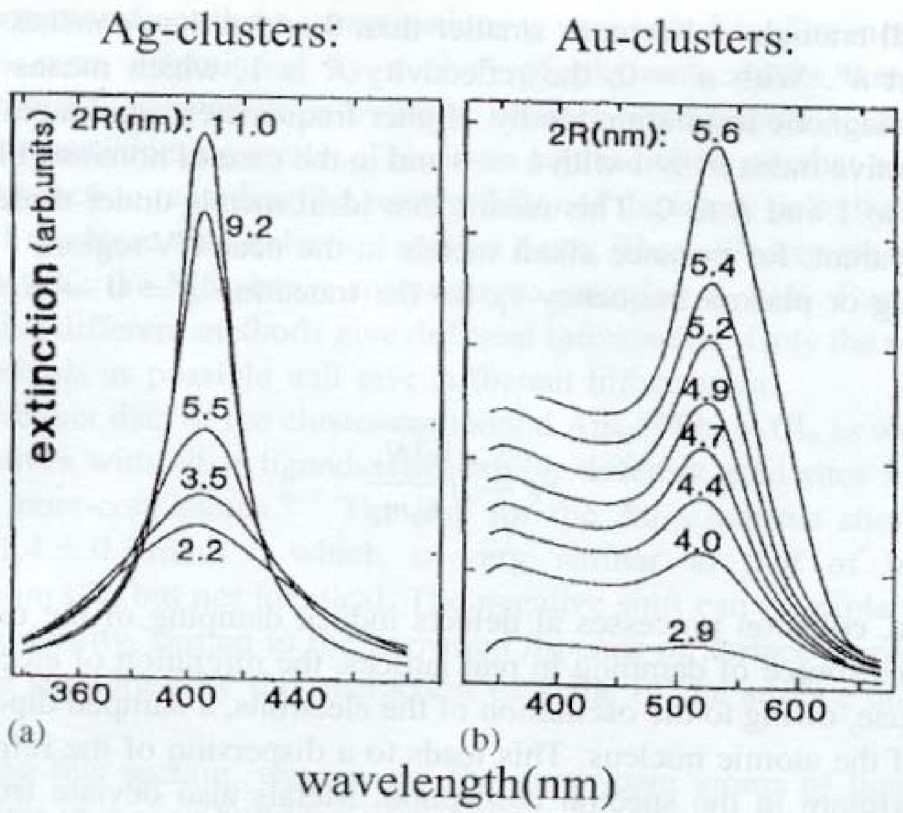

FIGURE 2.10 Absorbance spectra of (a) silver and (b) gold clusters of different sizes. Reprinted with permission from *Handbook of Optical Properties*, Vol. II (ed Hummel and Wissmann) 1997. Copyright CRC Press, Boca Rata, Florida.[12]

Light-induced transition between these levels determines the color of the materials

UV photo-electron spectroscopy

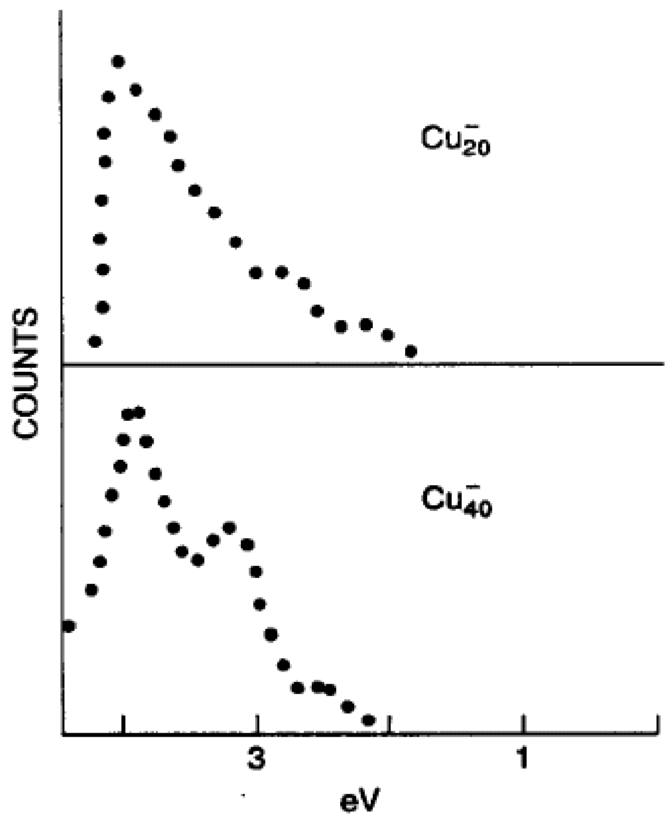

Figure 4.11. UV photoelectron spectrum in the valence band region of copper nanoparticles

4.2.5 Reactivity

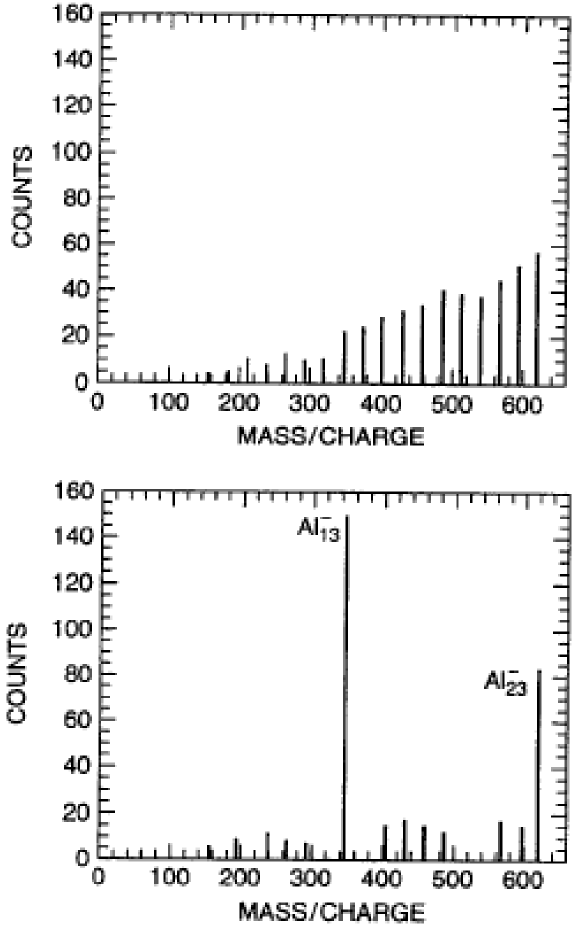

Figure 4.13. Mass spectrum of Al nanoparticles before (top) and after (bottom) exposur oxygen gas. [Adapted from R. E. Leuchtner et al., *J. Chem. Phys.*, **91**, 2753 (1989).]

4.2.6 Fluctuations ?

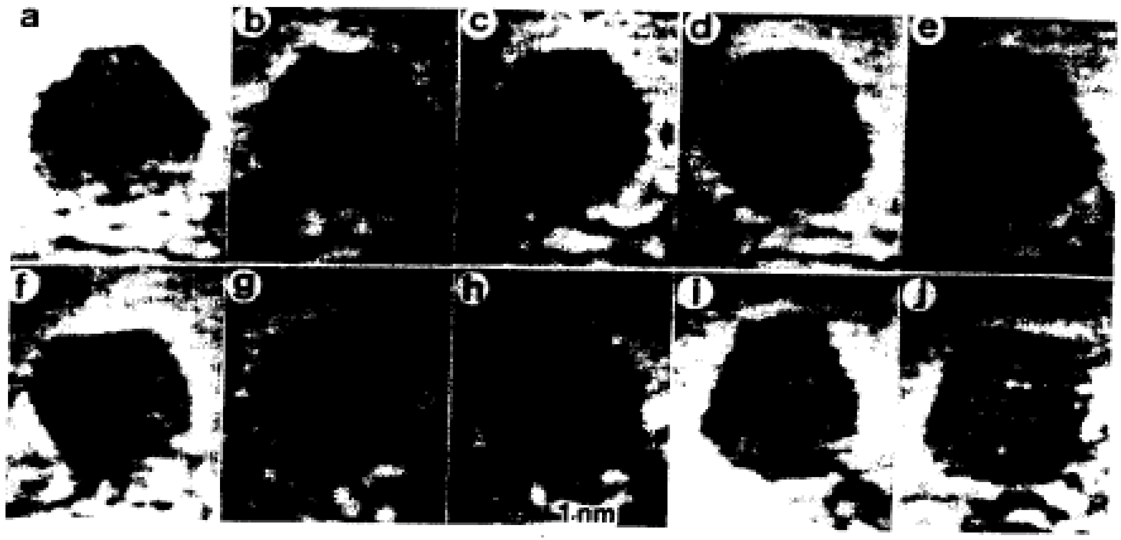

Figure 4.15. A series of electron microscope pictures of gold nanoparticles containing approximately 460 atoms taken at various times showing fluctuation-induced changes in the structure. (With permission from S. Sugano and H. Koizumi, in *Microcluster Physics*, Springer, Berlin,

4.2.7 Magnetic cluster

- Magnetized cluster
- Nonmagnetic- magnetic transition

Superparamagnetism:

1. Orbital magnetic moment
2. Electron spin
3. Levels filled with an even number of electrons→ net magnetic moment=0
4. Transition ion atoms: Fe, Mn, Co with partially filled inner d-orbital levels-→
   net magnetic moment
   Parrel align   Ferromagnetic
5 Ferromagnetic cluster with DC field → superparamagnetism

Superparamagnetism

BASIS FERROMAGNETISM

Ferro-magnetisme:

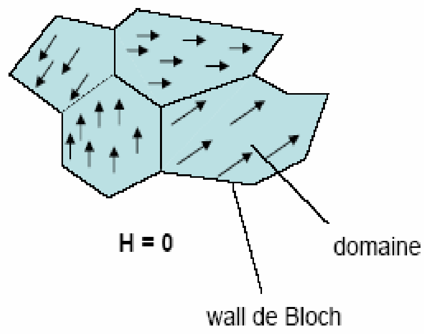

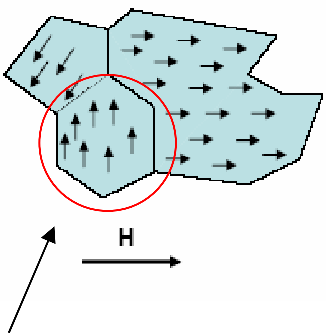

Single domain

Materials: Fe, Co, Ni, Gd

Spins of unfilled d-bands spontaneously align parallel inside a *domain* below a critical temperature T_C (Curie)

Laws:

$$B = H + 4\pi \cdot \chi \cdot H$$

$$M = \chi \cdot H$$

$$\chi = Susceptibility$$

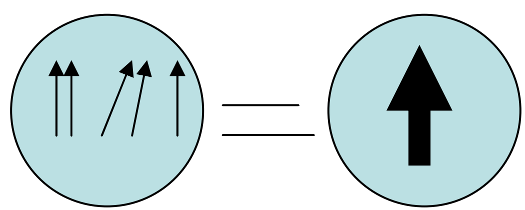

Superparamagnetism

⇒Particles with net moment(Ferromagnetic particles with moment ,Tc is high)

- Mono-domain when d < 100 nm

⇒Fluctuation of the magnetic moment like in a paramagnet

⇒Moment dependent on particle volume

此圖為$FeSi_2$奈米粉末的DC磁化率

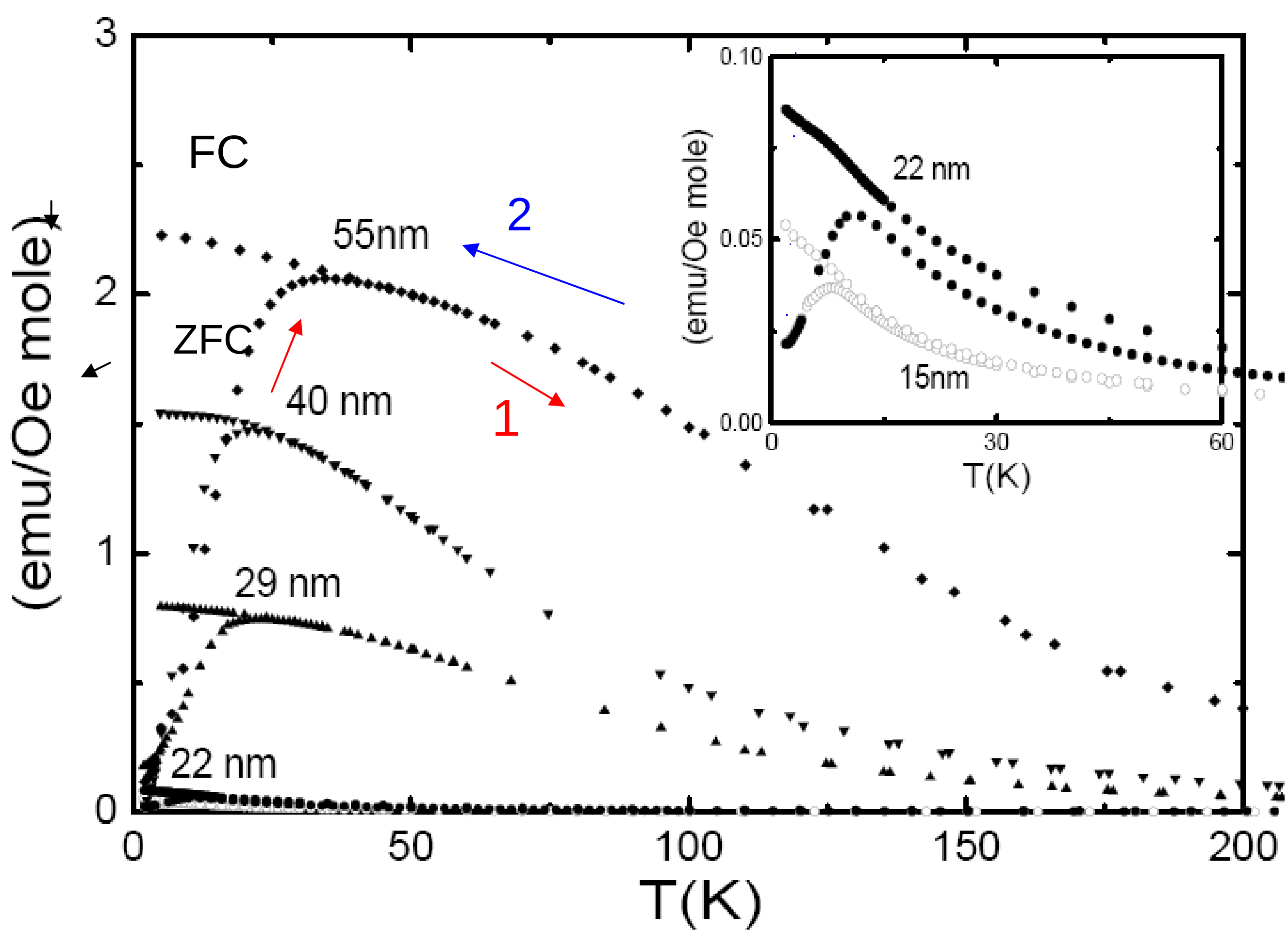

- 1. The temperature of peak value of χ in ZFC is defined as the Blocking temperature T_B。
- 2. χ of ZFC and χ of FC deviate at T_B
- 3. Above T_B, χ of ZFC and χ of FC are overlap.

Blocking Temperature

$$T_B = \frac{KV}{25k_B}$$

k_B is the Boltzmann constant
K is the anisotropic constant
V is the volume of nanoparticle

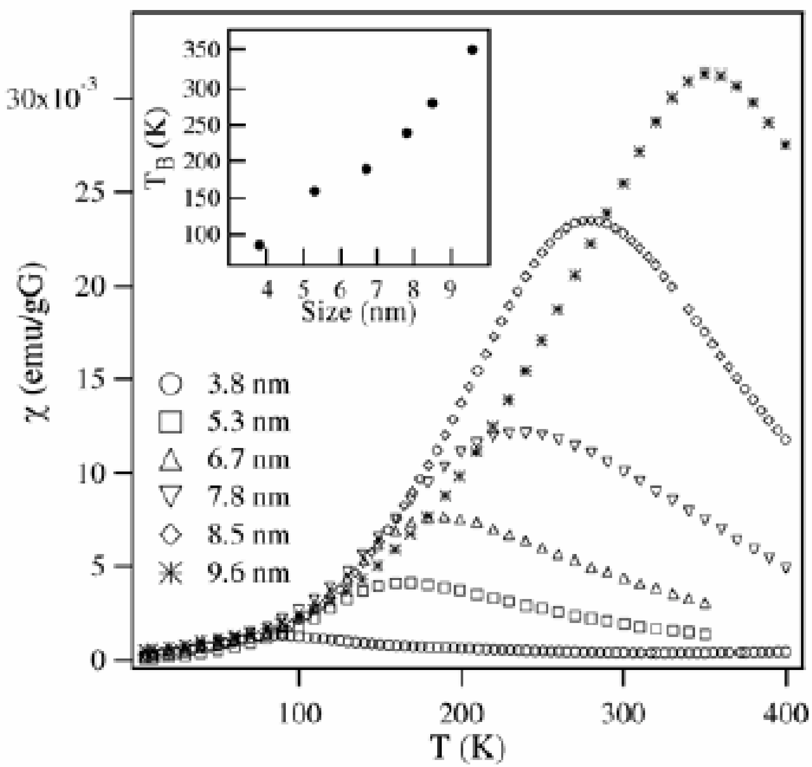

M-H曲線

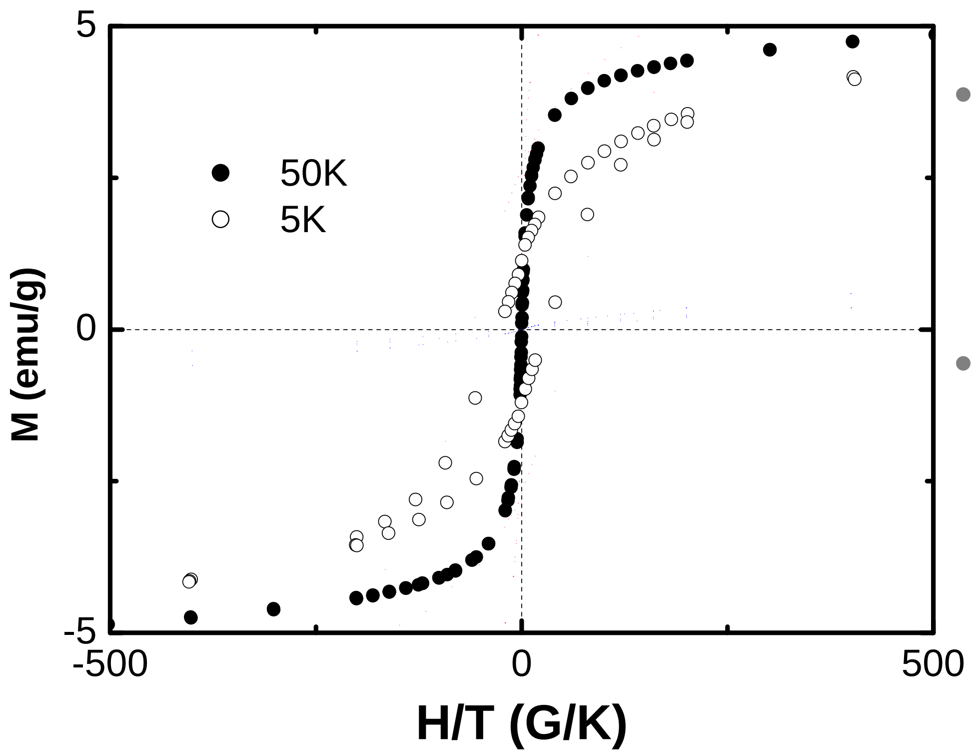

- 1. T< T_B, Hysteresis appears in M-H. Due to thermal energy is less than the interactions among particles
- 2. T> T_B, No hysteresis appears in M-H. Since thermal energy is larger than the interactions among particles

$FeSi_2$ 40nm particles T_B=20 K

Nonmagnetic- magnetic transition

4.2. METAL NANOCLUSTERS 89

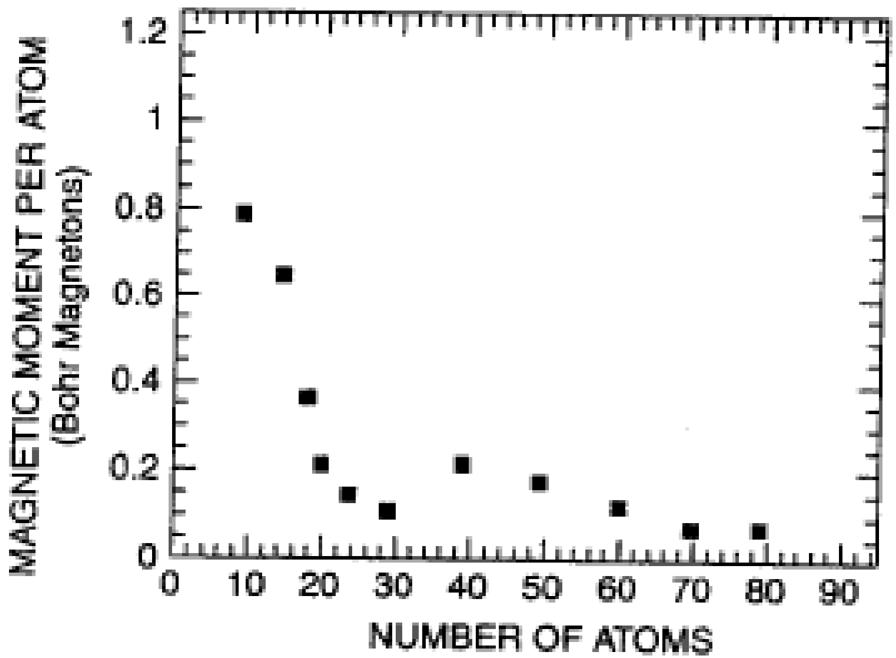

7. Plot of the magnetic moment per atom of rhenium nanoparticles versus the number

Rh

4.2.8 Bulk to Nanotransition

Gold melting point

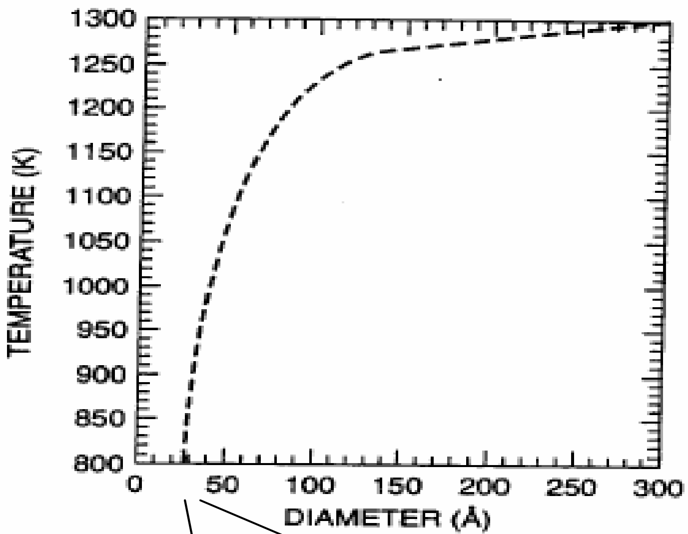

e 4.18. Melting temperature of gold nanoparticles versus particle diamete
ted from J. P. Borel et al., *Surface Sci.* **106**, I (1981).]

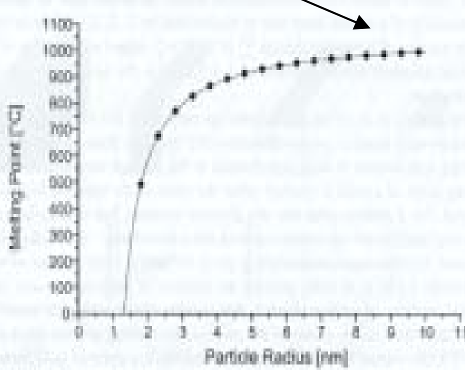

FIGURE 2.6 Relation between the size of gold particles and their melting point.

4.3 Semiconducting Nanoparticles

- 4.3.1 Optical Properties
- blue shift as size is reduced
- Due to band gap
- Exciton: bound electron-hole pair,produced by a photon having hv> gap
- Hydrogen-like: energy level spacing
- Light-induced transition

Hydrogen-like: energy level spacing
Light-induced transition

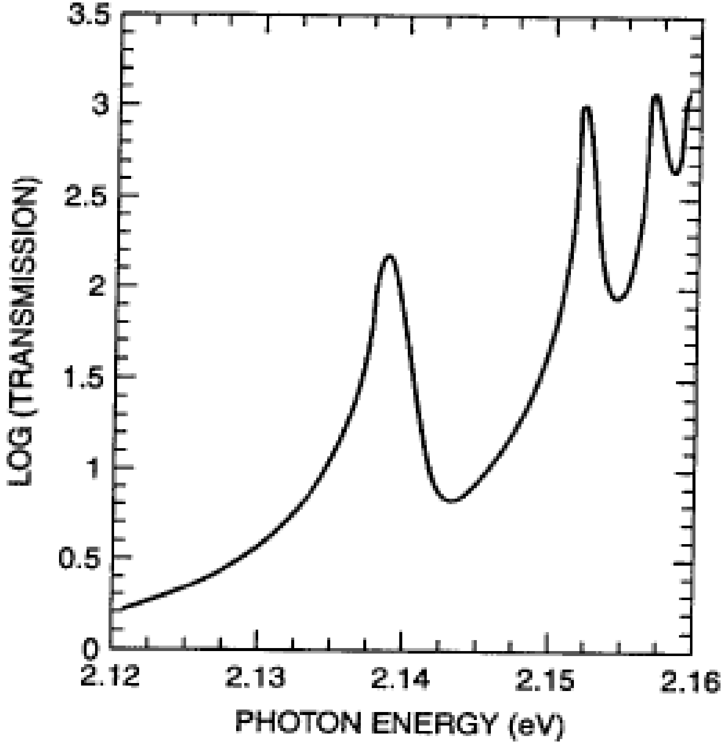

19. Optical absorption spectrum of hydrogen-like transitions of excitons in Cu_2O.
[From P. W. Baumeister, *Phys. Rev.* 121, 359 (1961).]

What happens when the size of nanoparticles becomes smaller than to the radius of the orbit of exciton?

- **Weak-confinement**
- size d> radius of electron-hole pair:
- blue shift
- **Strong-confinement**
- size d< radius of electron-hole pair:
- Motion of the electron and the hole become independent, the exciton does not exist

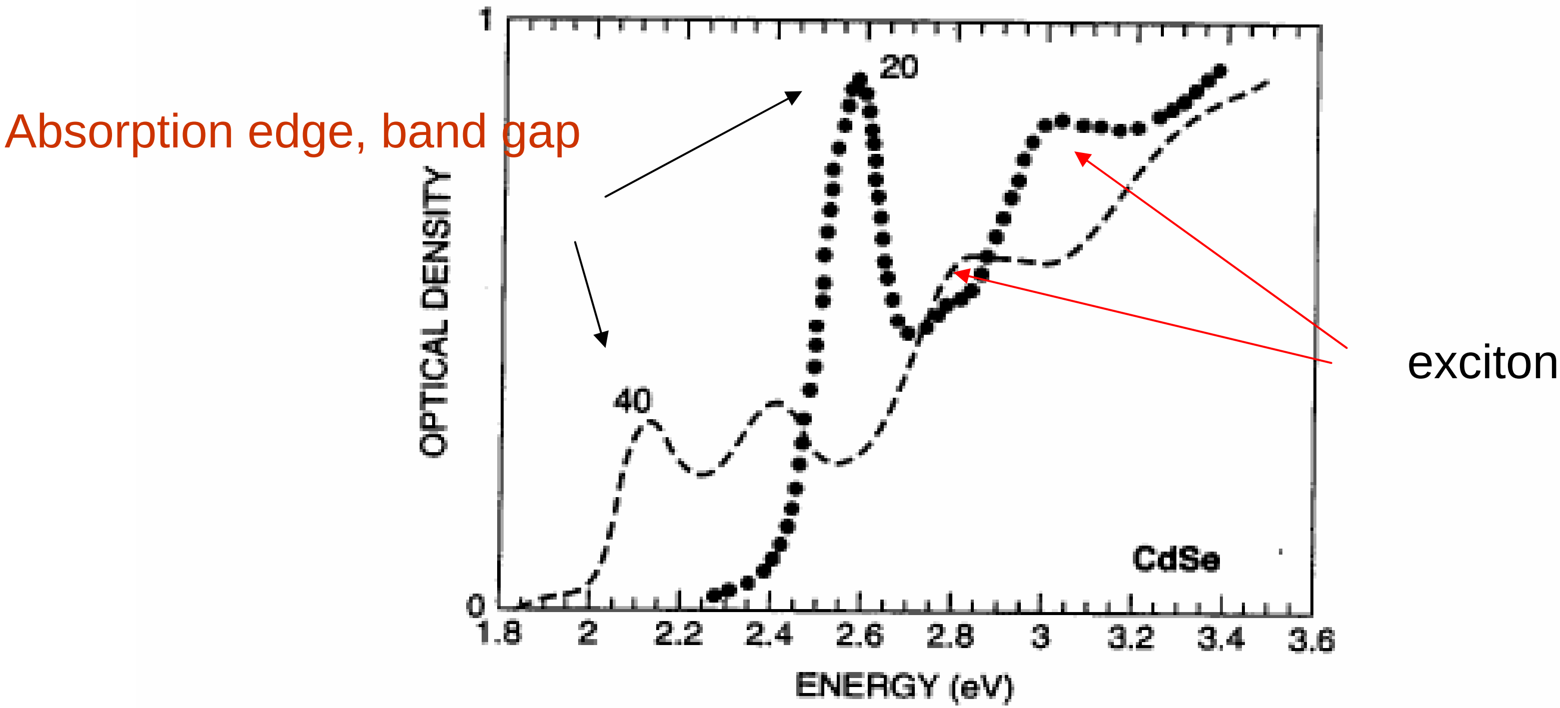

Figure 4.20. Optical absorption spectrum of CdSe for two nanoparticles having sizes 20 Å and 40 Å, respectively. [Adapted from D. M. Mittleman, *Phys. Rev.* **B49**, 14435 (1994).]

5. Size dependence properties of quantum dots CdSe –surface charge density

absorbance

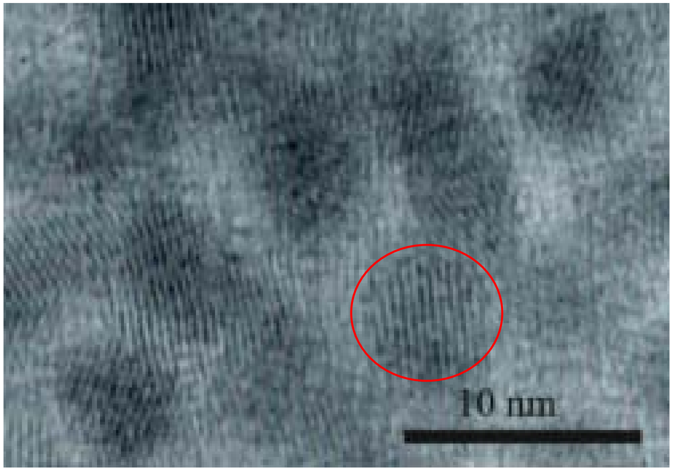

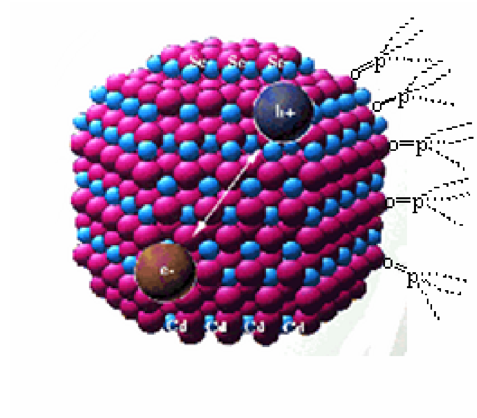

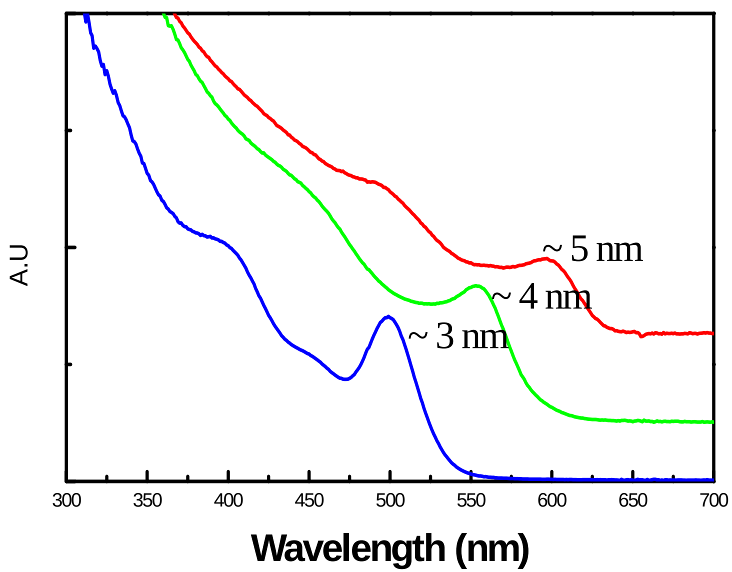

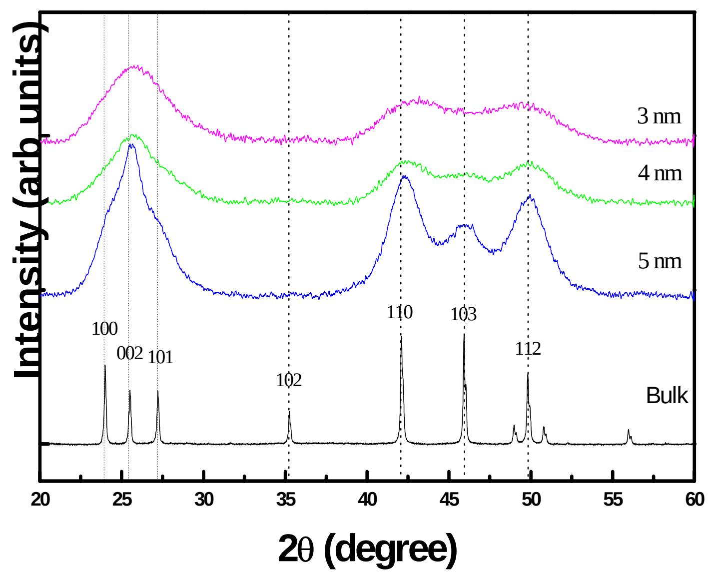

4.3.2 Photofragmentation

- Si or Ge can undergo fragmentation under laser light

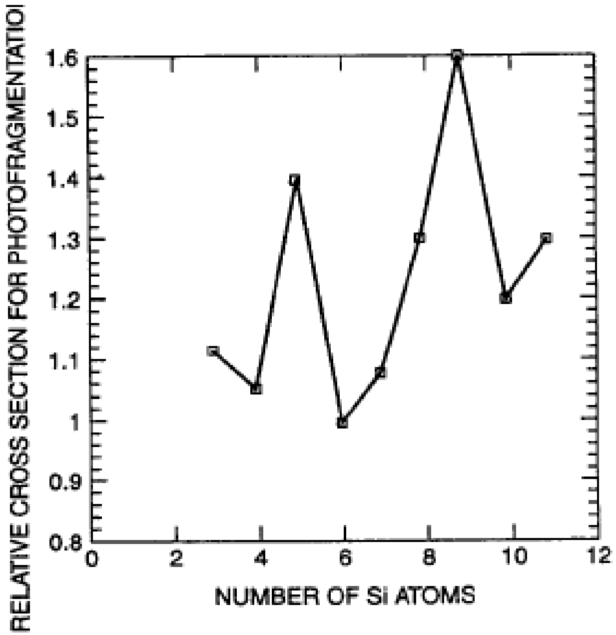

Figure 4.21. Photodissociation cross section of silicon nanoparticles versus number of atoms in particle. [Adapted from L. Bloomfield et al., *Phys. Rev. Lett.* **54**, 2266 (1985).]

Dissociate!

$$Si_{12} + h\nu \rightarrow Si_6 + Si_6 \quad (4.4)$$

$$Si_{20} + h\nu \rightarrow Si_{10} + Si_{10} \quad (4.5)$$

4.3.3 Coulombic Explosion

Multiple ionization of clusters causes them to become unstable, resulting in very rapid high-energy dissociation or explosion. The fragment velocities from this process are very high. The phenomena is called *Coulombic explosion*. Multiple ioniza-

Table 4.2. Some examples of the smallest obtainable multiply charged clusters of different kinds (smaller clusters will explode)

	Charge		
Atom	+2	+3	+4
Kr	Kr_{73}		
Xe	Xe_{52}	Xe_{114}	Xe_{206}
CO_2	$(CO_2)_{44}$	$(CO_2)_{106}$	$(CO_2)_{216}$
Si	Si_3		
Au	Au_3		
Pb	Pb_7		

$F=e^2/r2$

The attractive forces between the atoms of the cluster can be overcome by the electrostatic repulsion between the atoms when they become positively charged as a result of photoionization. One of the most dramatic manifestations of Coulombic explosion reported in the journal *Nature* is the observation of nuclear fusion in deuterium clusters subjected to femtosecond laser pulses. A femtosecond is 10^{-15} seconds. The clusters were made in the usual way described above, and then subjected to a high-intensity femtosecond laser pulse. The fragments of the dissociation have energies up to one million electron volts (MeV). When the deuterium fragments collide, they have sufficient energy to undergo nuclear fusion by the following reaction:

$$D + D \Rightarrow {}^{3}He + \text{neutron} \qquad (4.6)$$

This reaction releases a neutron of 2.54 MeV energy. Evidence for the occurrence of

4.4 Rare Gas and Molecular Clusters

- 4.4.1
- Xenon clusters are formed by adiabatic expansion of a supersonic jet of the gas through a small capillary into a vacuum.

Xenon having 13, 19, 25, 55, 71, 87, and 147 atoms.

$$U(R) = \frac{B}{R^{12}} - \frac{C}{R^{6}}$$

Lennard-Jones potential for calculation structure

Repulsion of coulombic electronic core

Dipole attractive potential

4.4.2 Superfluid Clusters

- By supersonic free-jet expansion
- He4 : N=7,10,14,23,30
- He3: N+ 7,10,14,21,30

- Superfluidity:
- He N=64,128
- Fermion has half-integer spin

  Boson has integer spin

difference. The case where all the bosons are in the lowest level is referred to as *Bose–Einstein condensation*. When this occurs the wavelength of each boson is the same as every other, and all of the waves are in phase.

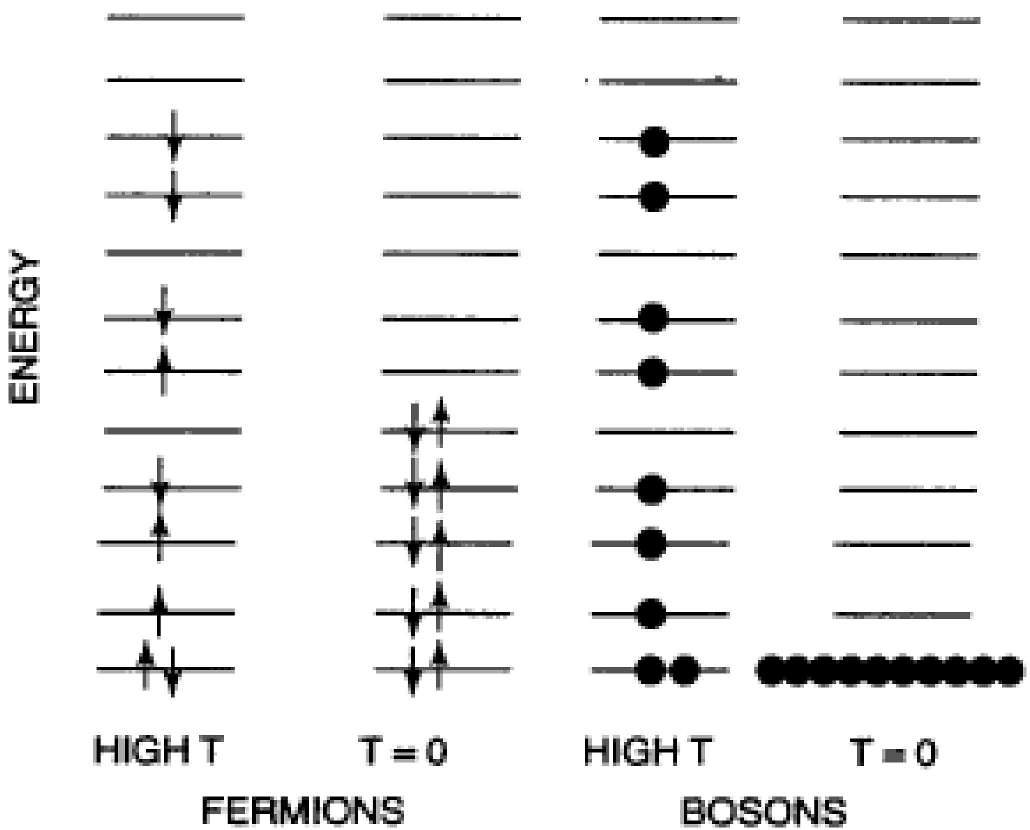

Figure 4.22. Illustration of how fermions and bosons distribute over the energy levels of a system at high and low temperature.

superfluid

- When T= 2.2 K lambda point
- He4 becomes a superfluid, its viscosit drops to zero

When boson condensation occurs in liquid He^4 at the temperature 2.2 K, called the *lambda point* (λ point), the liquid helium becomes a superfluid, and its viscosity drops to zero. Normally when a liquid is forced though a small thin tube, it moves

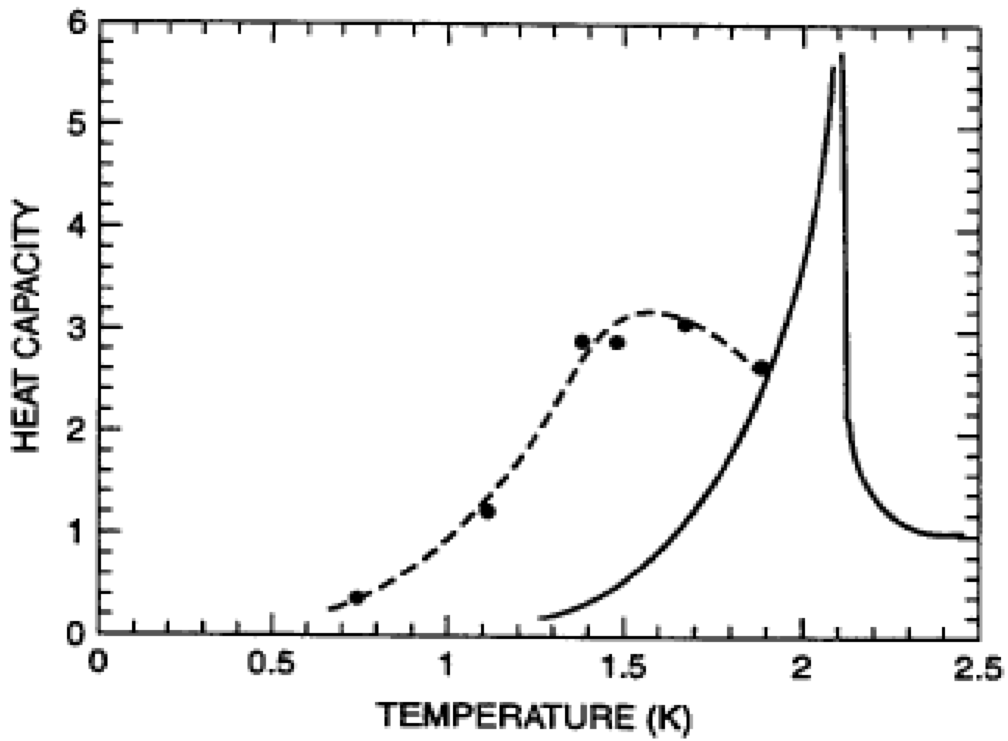

Figure 4.23. Specific heat versus temperature for liquid helium (solid line) and a liquid consisting of clusters of 64 helium atoms (dark circles). The peak corresponds to the transition to the superfluid state. [Adapted from P. Sindzingre, *Phys. Rev. Lett.* 63, 1601 (1989).]

P. Sindzingre PRL 63,1061(1989)

Path-Integral Monte Carlo Study of Low-Temperature ^{4}He Clusters

Philippe Sindzingre and Michael L. Klein
Department of Chemistry, University of Pennsylvania, Philadelphia, Pennsylvania 19104-6323

David M. Ceperley
National Center for Supercomputer Applications, Department of Physics, University of Illinois, Champaign, Illinois 61820
(Received 12 July 1989)

Path-integral Monte Carlo calculations have been used to study ^{4}He clusters at low temperatures. We develop a fluctuation formula for the superfluid fraction in terms of a projected area swept out by a path. Manifestations of superfluid behavior are shown to exist in a cluster of 64 atoms and a remnant of the λ transition persists in a cluster of 128 atoms. The temperature dependence of the superfluid fraction is similar to that observed in the liquid.

PACS numbers: 67.40.−w, 36.40.+d

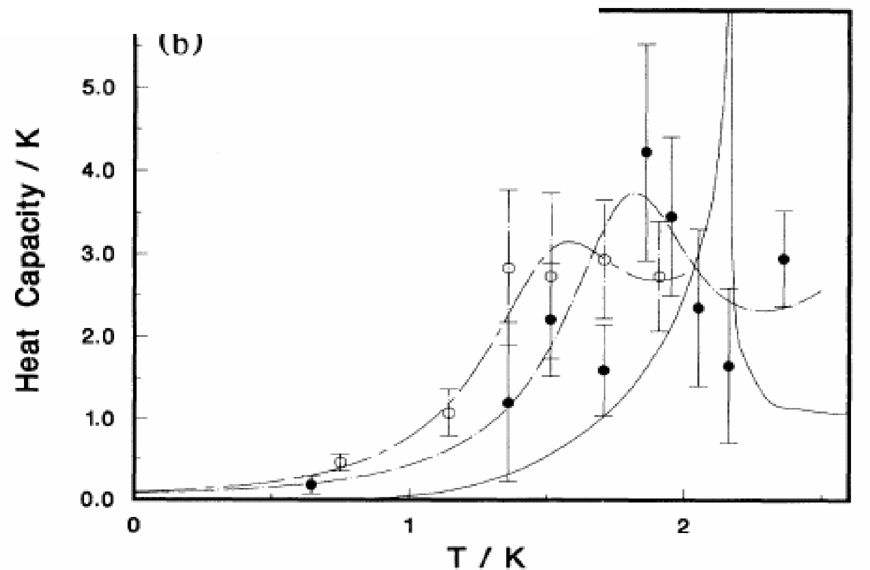

FIG. 1. Path-integral results for the (a) energy and (b) heat capacity of ^{4}He clusters with $N=64$ (open circles) and 128 (solid circles). The $T=0$ K energy values were taken from Green's-function Monte Carlo calculations (Ref. 2). The solid line refers to the bulk heat capacity (Ref. 11) and other lines are drawn as a guide to the eye.

4.4.3. Molecular Clusters

Individual molecules can form clusters. One of the most common examples of this is the water molecule. It has been known since the early 1970s, long before the invention of the word *nanoparticle*, that water does not consist of isolated H_2O molecules. The broad Raman spectra of the O–H stretch of the water molecule in the liquid phase at 3200–3600 cm^{-1} has been shown to be due to a number of overlapping peaks arising from both isolated water molecules and water molecules hydrogen-bonded into clusters. The H atom of one molecule forms a bond with the

At ambient condition
80% of water moleculars
Are bounded into clusters

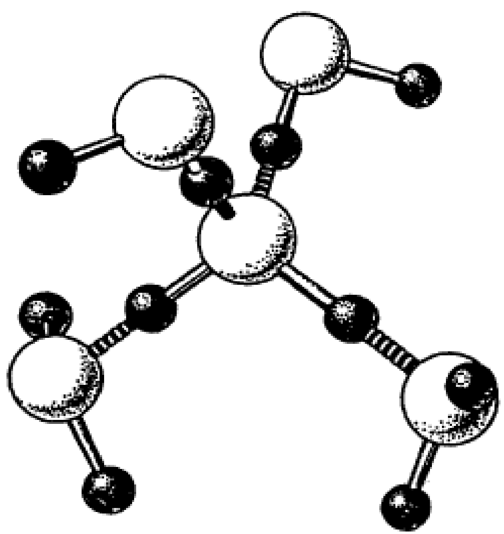

Figure 4.24. A hydrogen-bonded cluster of five water molecules. The large spheres are oxygen, and the small spheres are hydrogen atoms.

4.5 Method of Synthesis

- 1. RF Plasma
- 2. Chemical Methods
- 3. Thermolysis
- 4. Pulsed Laser Methods

4.5.1 RF Plasma

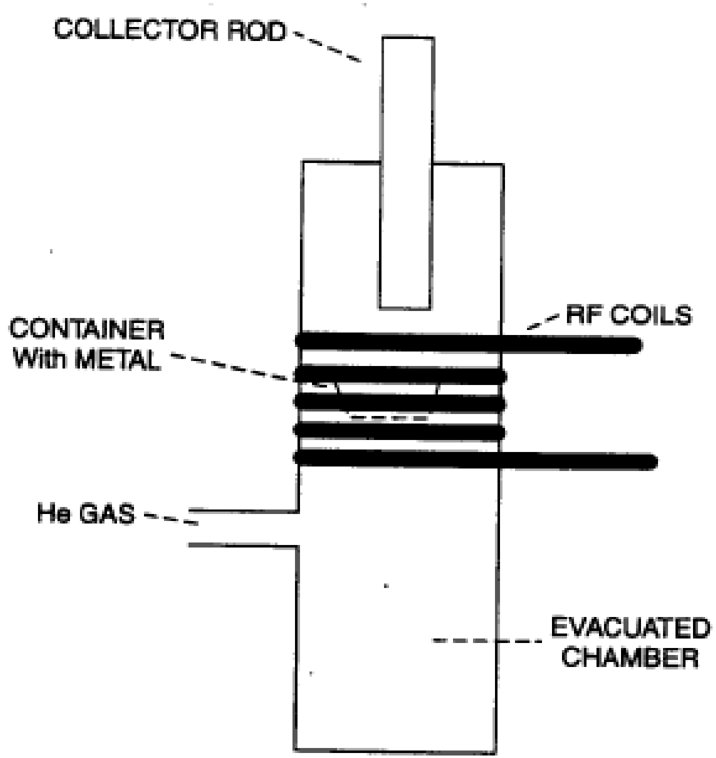

Figure 4.25. Illustration of apparatus for the synthesis of nanoparticles using an RF-produced plasma.

4.5.2 Chemical Method

Reducing agents

$$MoCl_3 + 3NaBEt_3H \Rightarrow Mo + 3NaCl + 3BEt_3 + (3/2)H_2 \qquad (4.9)$$

Nanoparticles of aluminum have been made by decomposing $Me_2EtNAlH_3$ in toluene and heating the solution to 105°C for 2 h (Me is methyl, $\cdot CH_3$). Titanium

4.5.3. Thermolysis(Thermal decomposition)

LiN_3-> Li

thermolysis. For example, small lithium particles can be made by decomposing lithium azide, LiN_3. The material is placed in an evacuated quartz tube and heated to 400°C in the apparatus shown in Fig. 4.26. At about 370°C the LiN_3 decomposes,

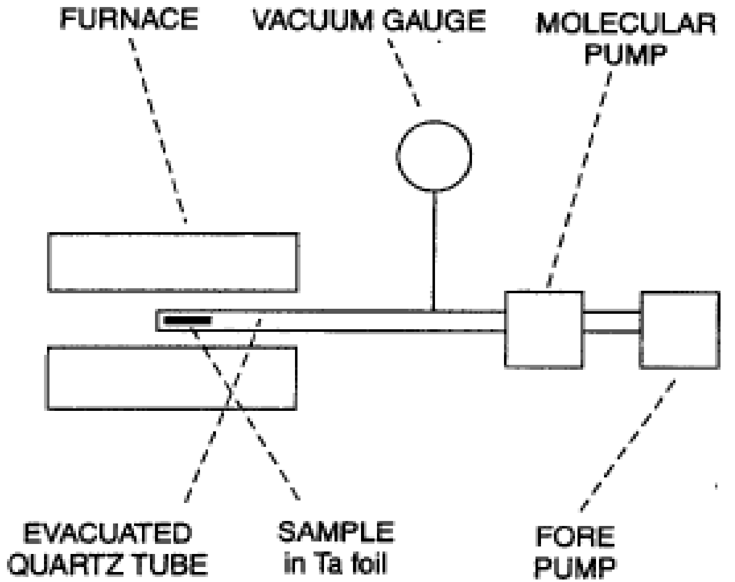

Figure 4.26. Apparatus used to make metal nanoparticles by thermally decomposing solids consisting of metal cations and molecular anions, or metal organic solids. (F. J. Owens, unpublished.)

Electron paramagnetic resorance (EPR)

- EPR measures the energy absorbed when electromagnetic radiation such as microwave induces a transition between the spin states m_s split by a DC magnetic field.

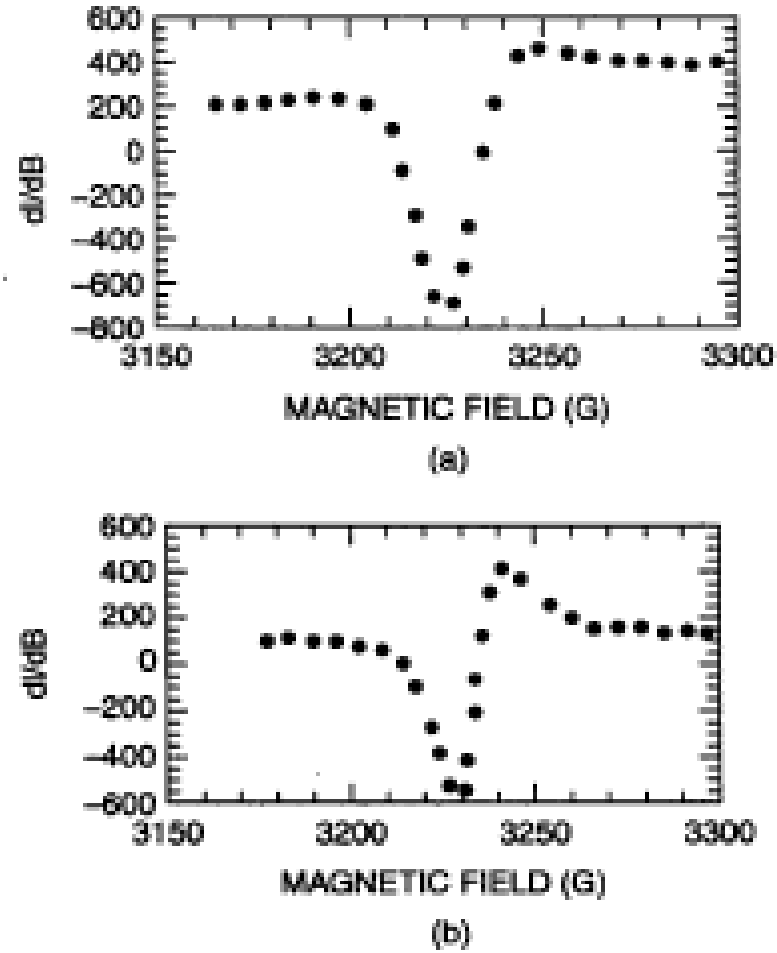

Figure 4.27. Electron paramagnetic resonance spectra at 300 K (a) and 77 K (b) arising from conduction electrons in lithium nanoparticles formed from the thermal decomposition of LiN_3. (F. J. Owens, unpublished.)

4.5.4 Pulsed Laser Method

Silver nitrate+ reducing agent -----> Silver nanoparticle

heating

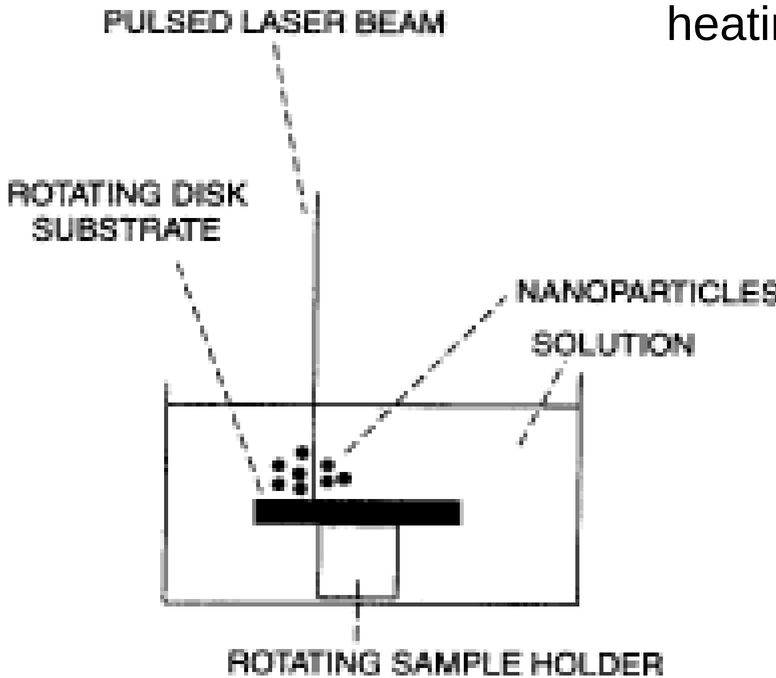

Figure 4.28. Apparatus to make silver nanoparticles using a pulsed laser beam that creates hot spots on the surface of a rotating disk. [Adapted from J. Singh, *Mater. Today* 2, 10 (2001).]

Laser Ablation

Laser Ablation

1. Quantum size effects on the competition between Kondo interaction and magnetic order in 0-D.

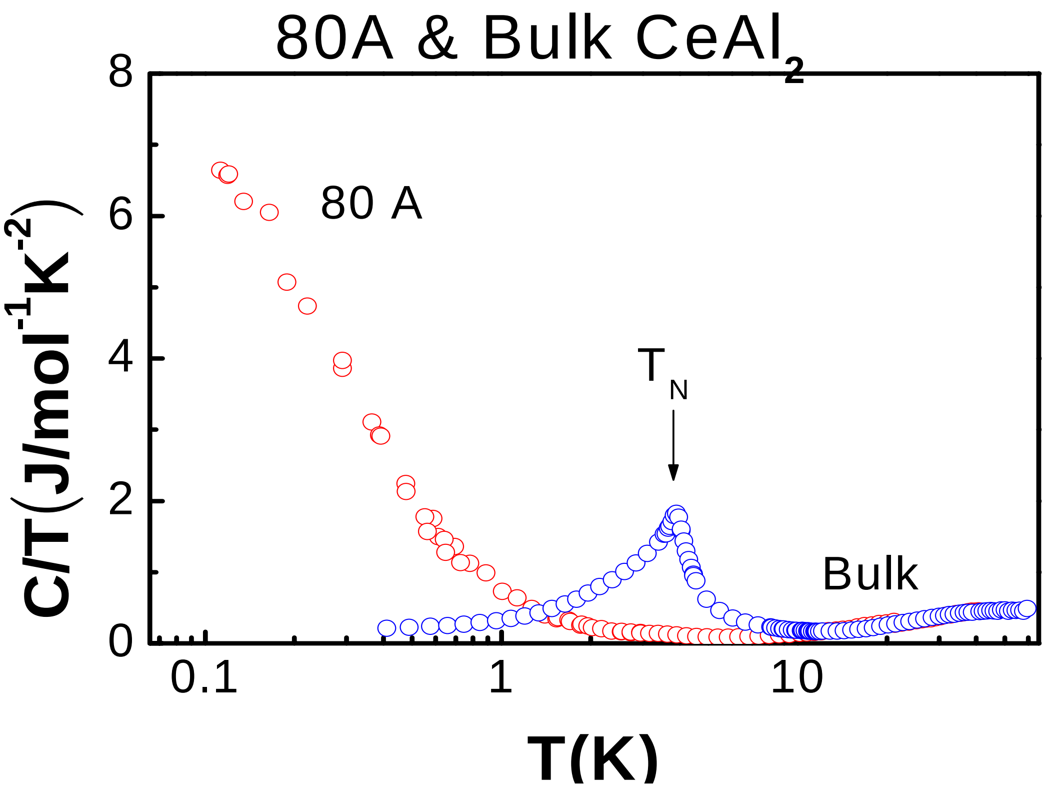

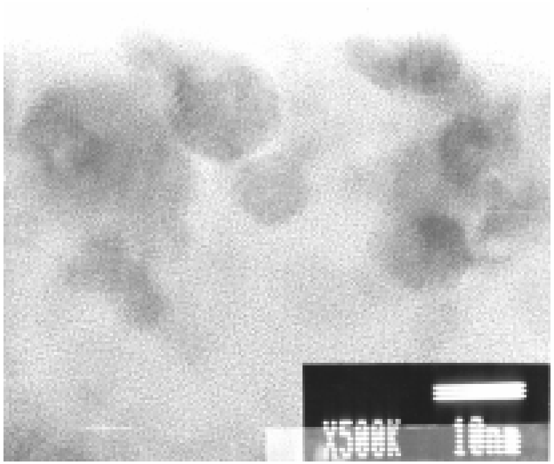

Conclusion:

In 80A -$CeAl_2$, magnetic ordering completely disappears and the γ reaches 9500 mJ/mol Ce K^2.

Unsolved problems:

In nanoparticle, only 0.7 Mole Ce^{3+} left, Is the 0.3 mol non-magnetic Ce really on the surface ? or it is just a coincidence.

Size dependence of Kondo effects in $CePt_2$ **nanoparticles**

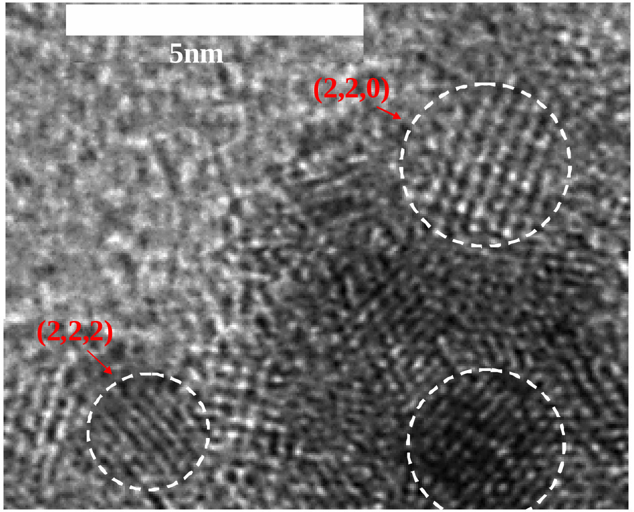

TEM of nanoparticles

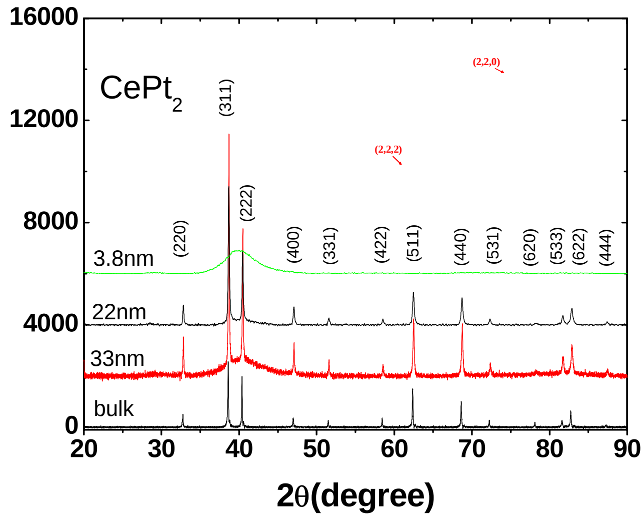

X-ray spectra

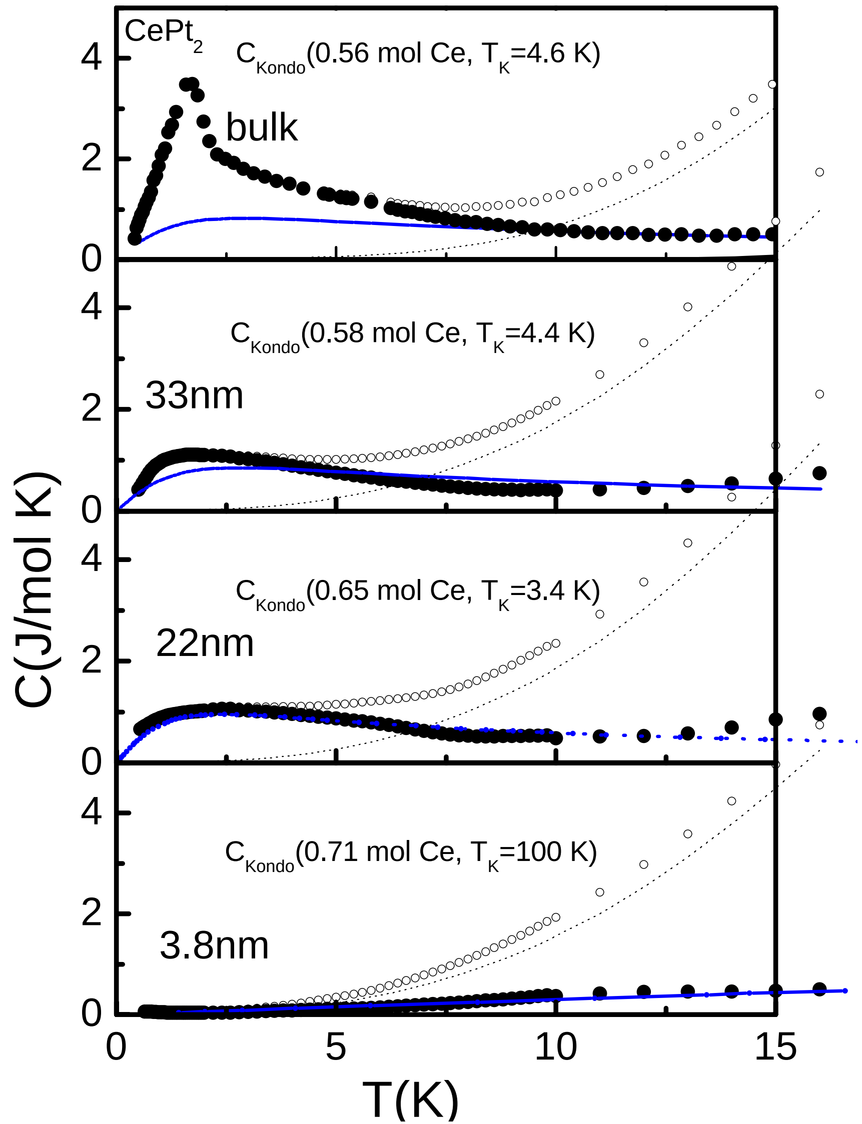

Specific heat of CePt2

4.6 Conclusion

In this chapter a number of examples have been presented showing that the physical, chemical, and electronic properties of nanoparticles depend strongly on the number and kind of atoms that make up the particle. We have seen that color, reactivity, stability, and magnetic behavior all depend on particle size. In some instances entirely new behavior not seen in the bulk has been observed such as magnetism in clusters that are constituted from nonmagnetic atoms. Besides providing new